ACS Catalysis

Research Article

Cite This: ACS Catal. 2018, 8, 2760−2773

pubs.acs.org/acscatalysis

Mechanistic Insights into One-Step Catalytic Conversion of Ethanol to Butadiene over Bifunctional Zn−Y/Beta Zeolite

Tingting Yan,[†] Weili Dai,*[,†,‡] Guangjun Wu,[†] Swen Lang,[§] Michael Hunger,[§] Naijia Guan,[†] and Landong Li*[,†,‡]

[†]School of Materials Science and Engineering & National Institute for Advanced Materials, Nankai University, Tianjin 300350, P.R. China

[‡]Key Laboratory of Advanced Energy Materials Chemistry of the Ministry of Education, Collaborative Innovation Center of Chemical Science and Engineering, Nankai University, Tianjin 300071, P.R. China

[§]Institute of Chemical Technology, University of Stuttgart, 70550 Stuttgart, Germany

Supporting Information

ABSTRACT: Bifunctional Zn−Y/Beta catalyst was applied in the reaction mechanism study of the ethanol to butadiene conversion to clarify the roles of Zn and Y functional sites in each individual reaction step. According to the results of several complementary methods, i.e., ethanol temperature-programmed desorption (TPD), temperature-programmed surface reaction (TPSR), and in situ diffuse reflectance infrared Fourier transform spectroscopy (DRIFTS), the reaction network consisting of several key steps, i.e., ethanol dehydrogenation, acetaldehyde aldol condensation, and crotonaldehyde reduction, was elucidated. An enolization mechanism was verified to involve in the coupling step. During this reaction, the Lewis acidic Zn and Y species in [Si]Beta zeolite were both active in the ethanol dehydrogenation, aldol condensation, and Meerwein−Ponndorf−Verley reduction. In this cycle, Zn species exhibited the higher dehydrogenation activity but lower coupling activity than that of Y species. Through the combination of the two species in one catalyst, i.e., Zn−Y/Beta, the synergistic effect of the bifunctional sites could be achieved. Our study provides mechanistic insights into the cascade transformation of ethanol to butadiene and the fundamental guidelines for the rational design of eligible catalysts for the reaction.

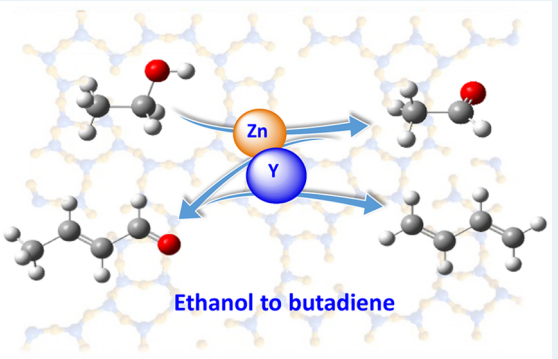

KEYWORDS: *ethanol to butadiene, reaction mechanism, bifunctional catalyst, synergistic effect, Lewis acid sites*

1. INTRODUCTION

As an important petrochemical intermediate, 1,3-butadiene is mainly used for the production of synthetic rubber, nylon intermediate adipnitrile, and also applied in the Diels−Alder reaction to form cycloalkanes and cycloalkenes.[1−3] Currently, butadiene is mainly obtained as a byproduct in the ethene production via naphtha steam cracking.[4] However, the recent use of shale gas for the production of ethene, instead of the steam cracking route, shows significant impact on the butadiene supply. Therefore, an alternative route to produce butadiene is highly desirable. With the recent increase in ethanol production, especially the rapid development of bioethanol, the interest in an ethanol to butadiene (ETB) process has been sparked again.[5−8]

Generally, two different approaches have been utilized for the ETB conversion. In the one-step process, ethanol is directly used as a feedstock over the bifunctional catalysts consisting of the dehydrogenation sites and the Lewis acid sites, e.g., MgO-SiO_2.[9−14] In the industrial two-step process, the co-feeding of acetaldehyde is indispensable because the Lewis acid sites, e.g., the supported metal oxides (Zr/SiO_2 or Ta/SiO_2) or heteroatom substituted zeolites (Zr-Beta or Ta-Beta),[2,15−19] cannot efficiently catalyze the dehydrogenation of ethanol to acetaldehyde. Recent studies revealed that by the introduction of dehydrogenation sites (Ag or Cu) into Lewis acidic catalysts, e.g., Zr-Beta or Ta-Beta, a two-step ETB catalyst can be transferred to a one-step ETB catalyst.[20−22] This method was also be expanded to the traditional one-step MgO-SiO_2 catalyst,[23−29] and in both cases, an enhanced yield of butadiene could be achieved.

Despite of the significant achievements made so far, the fundamental understandings of the ETB mechanism and the structure−activity relationship are still being explored. Through extensive debates in the past decades, several key reaction steps are now generally accepted (Scheme 1), including (i) the dehydrogenation of ethanol to acetaldehyde, (ii) the aldol condensation of acetaldehyde to acetaldol, (iii) the dehydration of acetaldol to crotonaldehyde, (iv) the Meerwein−Ponndorf−

Received: January 2, 2018
Revised: February 21, 2018
Published: February 22, 2018

© XXXX American Chemical Society

DOI: 10.1021/acscatal.8b00014
ACS Catal. 2018, 8, 2760−2773

Scheme 1. Reaction Network of Ethanol-to-Butadiene Conversion

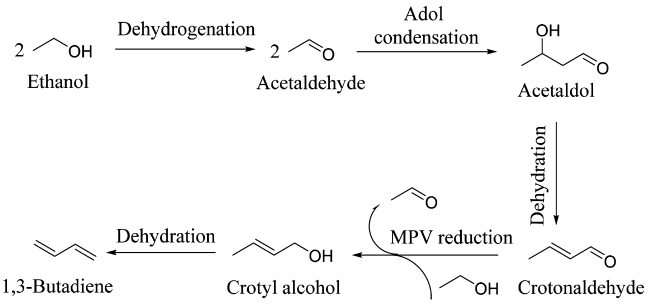

Verley (MPV) reduction of crotonaldehyde to crotyl alcohol, and (v) the dehydration of crotyl alcohol to butadiene.[1,5] On the basis of this reaction route, two independent catalytic cycles of a one-step process were proposed by Sushkevich and Ivanova, i.e., dehydrogenation of ethanol into acetaldehyde over metal sites and acetaldehyde/ethanol transformation into butadiene at Lewis acid sites.[30] This is in line with the recent reports of Hermans and co-workers, where they suggested that Lewis acid sites in Zr-Beta or Ta-Beta catalysts were responsible for the acetaldehyde coupling,[2,31] while Ag metal only promoted the ethanol dehydrogenation to acetaldehyde.[31] In addition, Zn cations in the talc-Zn-modified catalysts were proved to accelerate the rate of ethanol dehydrogenation to acetaldehyde but had no influence on the formation of crotonaldehyde.[25]

The overall reaction route and the main reaction steps leading to butadiene are now solidly established. However, molecular-level insights into the mechanisms of each reaction step, especially the independent roles of the two different types of active sites, and whether the roles of two individual active sites will be influenced by each other after their combination in a bifunctional catalyst, are still missing now and are, therefore, the aims of this work.

In our previous work, we have demonstrated that the bicomponent Zn−Y clusters confined in [Si]Beta zeolite, i.e., the Zn−Y/Beta catalyst, exhibit a state-of-the-art butadiene selectivity of 81% or butadiene productivity of 2.33 $g_{butabiene}/(g_{cat}\cdot h)$.[32] In the present study, the independent roles of Zn and Y species in each reaction step of the ETB conversion and the mechanism of each step were investigated in detail. The acidity of Zn/Beta, Y/Beta, and Zn−Y/Beta catalysts were first studied by ^{1}H and ^{13}C MAS NMR spectroscopy with probe molecule adsorption. The catalytic performance of these catalysts was evaluated in a fixed-bed reactor. Then, ethanol-TPD, TPSR experiments, and in situ DRIFT spectroscopy were applied to monitor the dynamic changes on the catalyst surface as well as the product distribution in the gas phase simultaneously. Additionally, modulation experiments with acetaldehyde and crotonaldehyde co-feeding were applied to compare the roles of Zn and Y species in the ETB conversion. On the basis of the catalytic and spectroscopic results, the reaction mechanism and the roles of Zn and Y species during the ETB conversion can be well elucidated.

2. EXPERIMENTAL SECTION

2.1. Preparation of the Materials. Zn/Beta, Y/Beta, and Zn−Y/Beta catalysts were prepared by a two-step metalation procedure as described elsewhere.[32] Typically, the commercial H/[Al,Si]Beta zeolite (Sinopec Co.) with nominal n_{Si}/n_{Al} ratio of 13.5 was added to a 13 mol/L nitric acid aqueous solution and stirred for 20 h at 373 K to obtain a dealuminated [Si]Beta. The obtained product was separated by filtration and washed with deionized water until pH = 6−7. Then, the above sample was dried overnight at 473 K. Afterward, 1.0 g of the solid powder was mixed with metal nitrates (namely zinc nitrate or/and yttrium nitrate) and finely ground for 10 min and calcined at 823 K for 6 h. The final material was labeled by *x*%-metal/Beta (*x* refers to the weight loading), that is, 5%Zn/Beta, 5%Y/Beta, and 5%Zn-5%Y/Beta (hereinafter referred to Zn/Beta, Y/Beta, and Zn−Y/Beta). The as-obtained samples were directly utilized as catalysts in the ETB conversion.

2.2. Characterization of the Materials. The X-ray diffraction (XRD) patterns of samples were recorded on a Rigaku SmartLab powder diffractometer using Cu Kα radiation (λ = 1.5418 Å) with a scanning rate of 4°/min in the range of 2θ = 5−50°.

The surface areas and pore volumes of the calcined samples were measured by means of nitrogen adsorption on a Quantachrome iQ-MP gas adsorption analyzer at 77 K. Before the nitrogen adsorption, samples were dehydrated at 573 K for 6 h. The total surface area was calculated via the Brunauer−Emmett−Teller (BET) equation. The micropore size distribution was determined using the t-plot method.

The solid-state MAS NMR measurements were performed on a Bruker Avance III spectrometer at resonance frequencies of 400.1 and 100.6 MHz for ^{1}H and ^{13}C nuclei, respectively. ^{1}H MAS NMR spectra were obtained upon a single-pulse excitation of $\pi/2$ with pulse duration of 2.6 μs and a repetition time of 20 s, respectively. ^{13}C CPMAS NMR spectra were recorded applying cross-polarization (CP) with a contact pulse of 4 ms and a repetition time of 4 s. All ^{1}H and ^{13}C, MAS NMR studies were performed with dehydrated samples, which were treated at 723 K in vacuum (below 10^{-2} Pa) for 12 h. Thereafter, the probe molecules ammonia and acetone-2-^{13}C were loaded for further studies as described elsewhere.[33] For the adsorption of acetone-2-^{13}C (99.5% ^{13}C-enriched, Sigma-Aldrich) on the dehydrated materials, the sample tubes were connected with a vacuum line and the probe molecules were adsorbed at 40 mbar within 10 min. Subsequently, the acetone-2-^{13}C-loaded samples were evacuated ($p < 10^{-2}$ mbar) at 295 K for 10 min to remove weakly physisorbed acetone-2-^{13}C. The ammonia loading of the dehydrated samples was done on a vacuum line by adsorption of 100 mbar ammonia (Griesinger) at 298 K for 10 min, followed by an evacuation ($p < 10^{-2}$ mbar) at 453 K for 2 h for removing weakly physisorbed ammonia.

2.3. Catalytic Reactions. The ETB conversion was performed in a fixed-bed reactor at atmospheric pressure. Typically, 0.3 g of the ETB catalyst (sieve fraction, 0.25−0.5 mm) was placed in a quartz reactor (5 mm i.d.) and pretreated in flowing nitrogen (20 mL/min) at 673 K for 1 h. After cooling to the desired reaction temperature of 623 K, ethanol was introduced into the system using a Shimadzu LC-20AT dual reciprocating plunger HPLC pump at a rate of 0.1−3 mL/h (diluted with 20 mL/min nitrogen as carrier gas) corresponding to the weight hourly space velocity (WHSV) of 0.3−7.9/h. The products were analyzed by an online chromatograph Shimadzu GC-2010 plus with flame ionization detector (FID) and a Poraplot Q-HT column (40 m × 0.18 mm × 0.18 μm). The possible gaseous products (H_2, CO, and CO_2) were monitored with a mass spectrometer (Pfeiffer Omnistar GSD 320).

DOI: 10.1021/acscatal.8b00014
ACS Catal. 2018, 8, 2760−2773

The ethanol conversion and butadiene selectivity are defined as follows:

$$\text{ethanol conversion (mol\%)} = \frac{[\text{ethanol}]_{\text{inlet}} - [\text{ethanol}]_{\text{outlet}}}{[\text{ethanol}]_{\text{inlet}}} \times 100\%$$

$$\text{butadiene selectivity (mol\%)} = \frac{2 \times [\text{butadiene}]_{\text{outlet}}}{[\text{ethanol}]_{\text{inlet}} - [\text{ethanol}]_{\text{outlet}}} \times 100\%$$

2.4. Ethanol Temperature-Programmed Desorption (TPD) and Surface Reaction (TPSR). Ethanol TPD and TPSR experiments were performed in the same temperature-programmed fixed-bed reactor (ut supra) connected with a downstream gas sampling mass spectrometer (MS, Pfeiffer-Balzer Omnistar). Typically, helium was utilized as the carrier gas because its lower m/z value of 4, which has no overlap with the main products or intermediates in the ethanol conversion.

For the ethanol TPD experiments, samples of ca. 0.3 g were pretreated at 723 K for 1 h in a helium flow (20 mL/min), cooled to 298 K, and loaded with ethanol for 20 min, using the helium as carrier gas. After that, the samples were purged with pure helium for 30 min to eliminate the physical absorbed ethanol at 298 K. Then, the ethanol-TPD experiment was carried out in the range of 298−723 K with a heating rate of 5 K/min. Compared with the ethanol TPD experiment, the only difference in the ethanol TPSR experiment is that ethanol was continuously introduced to the catalyst during increasing of reaction temperature from 298 to 723 K. To get more information about the reaction mechanism of the ETB conversion, ethanol and the main intermediates (see Scheme 1), including water, hydrogen, acetaldehyde, crotonaldehdye, crotonyl alcohol, and butadiene, were monitored by MS in the TPD and TPSR experiments. The m/z values of the above-mentioned species were referred as 46, 18, 2, 44, 70, 57, and 54, respectively.[2]

2.5. In Situ Diffuse Reflectance Infrared Fourier Transform Spectroscopy (DRIFTS). The organic intermediates formed during the ETB conversion process over the different catalysts was in situ monitored by DRIFTS as described in ref 34. The DRIFT spectra were recorded using a Bruker Tensor 27 spectrometer equipped with an in situ reaction chamber and a liquid N_2 cooled high sensitivity MCT detector. Prior to the FTIR studies, ca. 20 mg of the catalysts were finely ground and placed in the chamber. Then, the catalysts were activated in flowing argon gas at 673 K for 1 h and, subsequently, decreased to 623 K to collect the background spectra. After importing the background, the ethanol was fed into the chamber with WHSV = 1.0 h^{-1}, and time-resolved spectra were recorded with a resolution of 4 cm^{-1} and an accumulation of 128 scans.

3. RESULTS AND DISCUSSION

3.1. Physicochemical Properties of the Catalyst Materials. The possible structure changes of the Beta zeolites after the postsynthesis procedures were investigated by XRD, as shown in Supporting Information (SI) Figure S1. Typical diffraction lines characteristic of the BEA topology could be observed for all the samples, indicating that the primary BEA structure was well preserved after dealumination and Zn and/or Y introduction. These results are consistent with those from N_2 adsorption/desorption analysis, where no significant loss in surface areas and micropore volumes could be observed (SI Table S1). In addition, no obvious diffraction lines due to Zn and Y species occurred, indicating that the Zn and Y species were highly dispersed in Beta zeolite, which was supported by the STEM images of the Zn−Y/Beta sample in our previous report.[32]

The hydroxyl groups in [Si]Beta zeolites before and after the introduction of Zn and/or Y species were analyzed by ^{1}H MAS NMR spectroscopy. As shown in Figure 1, a dominant signal at

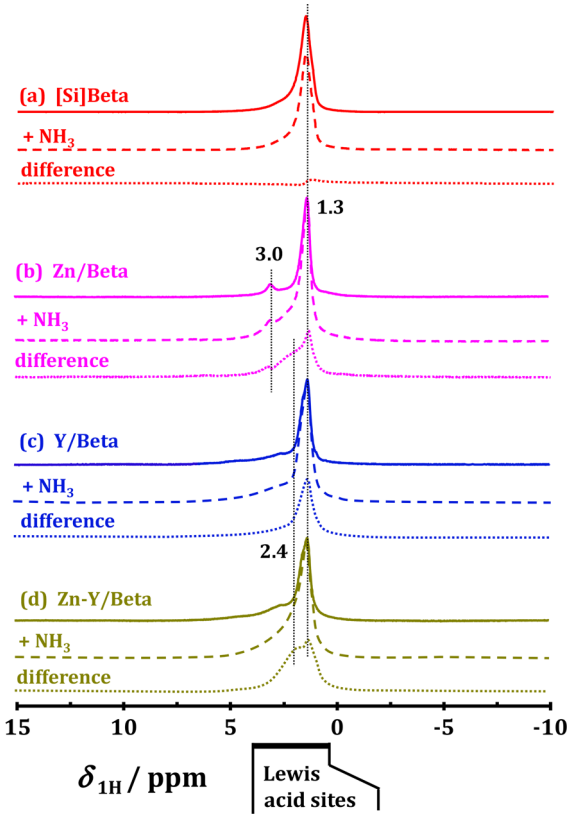

Figure 1. ^{1}H MAS NMR spectra of dehydrated [Si]Beta (a), Zn/Beta (b), Y/Beta (c), and Zn−Y/Beta (d) recorded before (top) and after (medium) adsorption of ammonia. The bottom spectra (difference) were obtained via subtracting the top spectra (dehydrated) from the medium spectra (after NH_3 adsorption).

δ_{1H} = 1.3 ppm due to silanol groups at framework defects occurred in all of the samples. After the introduction of Zn species, a new signal due to the Zn-OH group appeared at about δ_{1H} = 3.0 ppm,[35] which disappeared after the cointroduction of Y species. This indicates the interaction between Zn and Y species in the bifunctional Zn−Y/Beta catalyst, which is also supported by our previous XPS results.[32] After ammonia loading, nearly no changes of the ^{1}H MAS NMR spectra were observed for [Si]Beta, i.e., neither Brønsted nor Lewis acid sites were present in this material. On the other hand, a strong increase of the signal intensities in the shift range of δ_{1H} = 1.3−2.4 ppm occurred on Zn and/or Y modified Beta zeolites after ammonia loading. According to a previous report, these signals are due to ammonia molecules coordinated at Lewis acid sites.[36] These results evidence that the introduction of Zn or/and Y species into the [Si]Beta zeolite leads to the formation of Lewis acid sites. In addition, the absence of the ^{1}H MAS NMR signal of ammonium ions at about δ_{1H} = 6.4−6.7

DOI: 10.1021/acscatal.8b00014
ACS Catal. 2018, 8, 2760−2773

ppm for these ammonia-loaded samples exclude the formation of Brønsted acid sites after the introduction of Zn and/or Y species.

For additional evidence on the formation of Lewis acid sites on the catalysts under study, the adsorption of the probe molecule acetone-2-^{13}C on dehydrated samples was investigated by ^{13}C CP MAS NMR spectroscopy (Figure 2). For

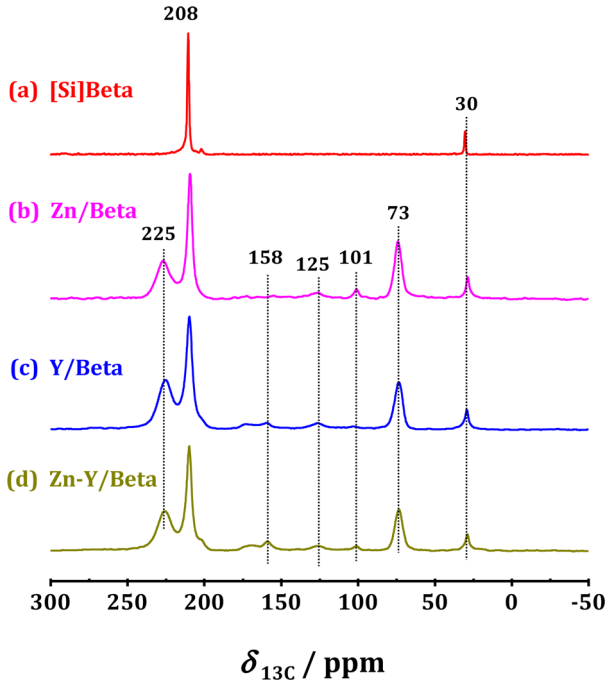

Figure 2. ^{13}C CPMAS NMR spectra of [Si]Beta (a), Zn/Beta (b), Y/Beta (c), and Zn−Y/Beta (d) recorded after adsorption of acetone-2-^{13}C.

[Si]Beta, the dominant signal at δ_{13C} = 208 ppm is due to physisorbed acetone-2-^{13}C at nonacidic silanol groups, while the weak signal at δ_{13C} = 30 ppm is assigned to non-^{13}C-enriched methyl groups of the probe molecules. After the introduction of Zn or/and Y species, new signals at about δ_{13C} = 225 appeared. These signals could be caused by strong Brønsted acid sites or the weak Lewis acid sites.[33,37] However, because of the absence of the ammonium signals at about δ_{1H} = 6.4−6.7 ppm in the ^{1}H MAS NMR spectra of the ammonia-loaded samples, an assignment of these signals to strong Brønsted acid sites could be excluded. Therefore, the signals at about δ_{13C} = 225 ppm in the spectra of the Zn and/or Y modified zeolites under study must be caused by acetone-2-^{13}C adsorbed at weak Lewis acid sits. In addition, signals at δ_{13C} = 73, 101, 125, and 158 ppm due to aldol condensation products of acetone are an indirect evidence for the presence of Lewis acid sites.[33] The appearance of signals at δ_{13C} = 158 ppm exclusively in the spectra of Y/Beta and Zn−Y/Beta indicates a higher aldol condensation activity of these catalysts in comparison with Zn/Beta.

Summarizing the characterization of surface sites by solid-state NMR spectroscopy, we come to the conclusion that the introduction of Zn and/or Y species in the [Si]Beta zeolite produces similar Lewis acid sites. Furthermore, Y species have demonstrated a higher aldol condensation activity in comparison with Zn species, which is very important for the ethanol to butadiene conversion (vide infra, Section 3.9).

3.2. Catalytic Performance of Zn and/or Y Modified Beta Catalysts in the ETB Conversion. As a very demanding reaction, the ETB conversion involves several key reaction steps (Scheme 1), and each step is catalyzed by a certain functional site. Therefore, multifunctional sites are required for an efficient ETB catalyst. For monometal-modified Beta zeolites, i.e., Zn/Beta and Y/Beta, low selectivity to butadiene was obtained, which slightly increased with the increasing ethanol conversion (Figure 3a). It means that the ETB conversion can be realized over Zn/Beta and Y/Beta catalysts. Hence, Zn and Y species both played bifunctional roles in the ETB conversion, but the individual Zn or Y species showed low efficiency for butadiene production. After the combination of Zn and Y species in joint surface sites, the catalytic performance of the ETB conversion was promoted, and the butadiene selectivity of ∼60% was

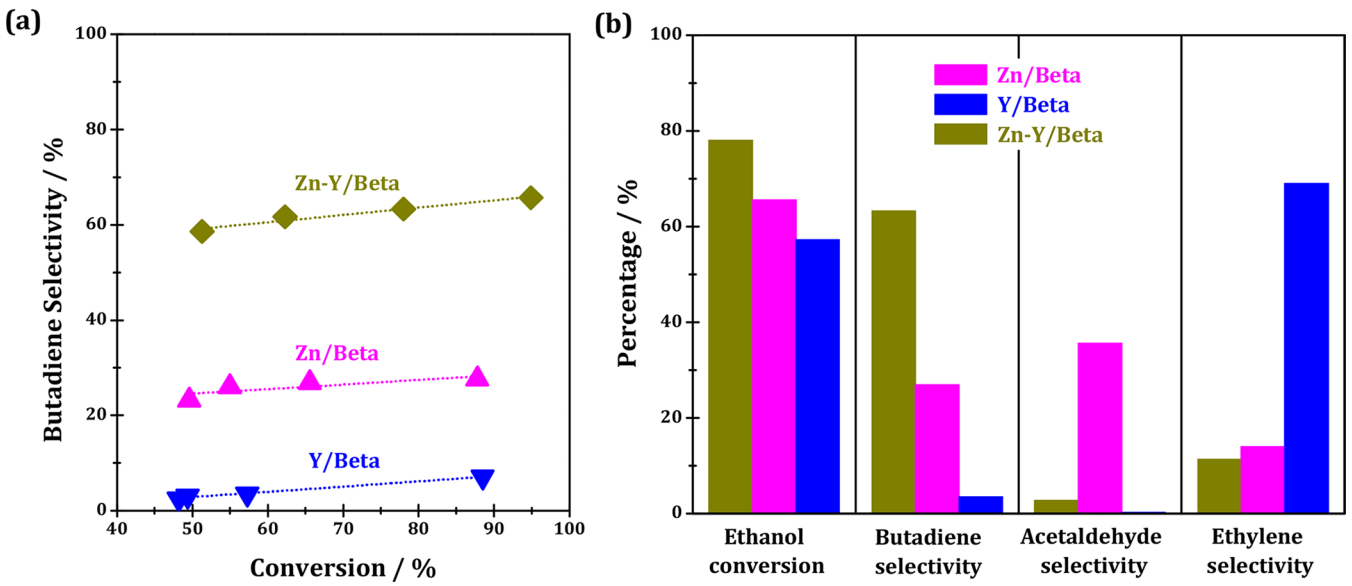

Figure 3. (a) Butadiene selectivity as a function of ethanol conversion over Zn/Beta, Y/Beta, and Zn−Y/Beta catalysts at 623 K with WHSV = 0.39−7.89 h^{-1} and (b) product distribution over Zn/Beta, Y/Beta, and Zn−Y/Beta catalysts under study at 623 K for WHSV = 1.0 h^{-1}.

DOI: 10.1021/acscatal.8b00014
ACS Catal. 2018, 8, 2760−2773

achieved over Zn−Y/Beta catalysts under employed reaction conditions. Obviously, the combination of Zn and Y species could play different roles in the ETB reaction cycle. According to the product distribution over Zn and Y/Beta catalysts (Figure 3b), Zn species appeared to be more active in the ethanol dehydrogenation to acetaldehyde because a large amount of acetaldehyde (S = 36%) was formed. On the other hand, Y species seemed to be more active in the acetaldehyde conversion because butadiene (S = ~5%) could be detected in the product while no acetaldehyde (S = 0%) was formed. Considering the similar Lewis acid sites existing in Zn/Beta, Y/Beta, and Zn−Y/Beta, their activity difference should be due to their functional sites and their interaction, which will be focused in the next sections.

3.3. Ethanol Temperature-Programmed Desorption (TPD) Experiments. To get more information about the reaction mechanism and the roles of Zn and Y species during the ETB conversion, several complementary experimental approaches were performed. First, ethanol TPD was utilized to investigate possible products or intermediates of this conversion. These intermediates monitored by MS, i.e., acetaldehyde (m/z = 44), crotonaldehyde (m/z = 70), crotonyl alcohol (m/z = 57), and butadiene (m/z = 54) were selected according to the mechanism proposed for ETB conversion (Scheme 1).[1,5,24,38,39] In addition to the m/z signals of the above-mentioned main intermediates, the m/z signals of hydrogen (m/z = 2), water (m/z = 18), and ethanol (m/z = 46) were monitored for comparison.

As demonstrated by the TPD-MS profiles in Figure 4, ethanol, water, acetaldehyde, and hydrogen were the major desorption products in the low-temperature range of 323−423 K for the three catalysts under study. This indicates that ethanol dehydration and dehydrogenation are the initial reaction steps during the ETB conversion at low reaction temperature. In the higher temperature range of 473−598 K, a higher content of hydrogen was observed for Zn/Beta than that for Y/Beta, indicating that Zn/Beta possessed higher dehydrogenation activity than Y/Beta. These results fit well with the catalytic results in Figure 3b, i.e., a higher selectivity to acetaldehyde obtained on Zn/Beta than that on Y/Beta. In addition, there were trace amounts of crotonaldehyde and crotyl alcohol with the same variation trend for all the three catalysts under study in the low-temperature range of 323−473 K. This is in good agreement with ETB reaction route (Scheme 1), which explains the formation of crotyl alcohol by a MPV reduction of crotonaldehyde. When the reaction temperature increasing to over 473 K, the amounts of crotonaldehyde and crotyl alcohol strongly increased, but the distributions of these two intermediates for the three catalysts under study were different. For Zn/Beta, crotonaldehyde was the dominant intermediate, while crotyl alcohol dominated for Y/Beta. After the combination of Zn and Y species to joint active sites, i.e., on Zn−Y/Beta, the amounts of crotonaldehyde and crotyl alcohol were very close. This illustrates that Y/Beta catalyst plays an essential role in the MPV reduction. Furthermore, two obvious desorption signals of butadiene could be observed for all three catalysts under study hinting at two different adsorption sites in these samples. The first desorption peak of butadiene for Y/Beta occurred at a slightly lower temperature than that for Zn/Beta, which might be explained by a weaker desorption energy of butadiene on Y/Beta compared with Zn/Beta. The temperature-programmed surface reaction experiments described in section 3.5, however, will demonstrate that a lower

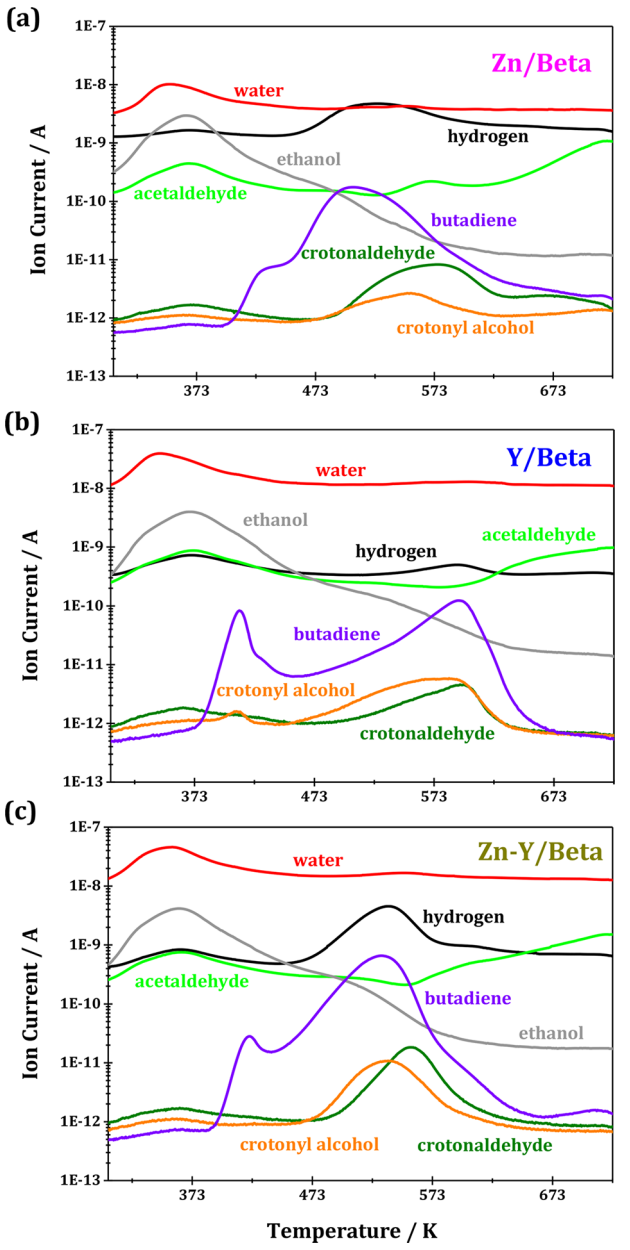

Figure 4. Temperature-programmed desorption of ethanol over Zn/Beta (a), Y/Beta (b), and Zn−Y/Beta (c) catalysts. Reaction conditions: WHSV = 1.0 h^{-1}, reaction temperature of T = 303−723 K.

formation temperature of butadiene occurs on Y/Beta, i.e. this catalyst reduces the activation energy barrier for the ETB conversion in comparison with Zn/Beta.

3.4. Temperature-Programmed Diffuse Reflectance Infrared Fourier Transform Spectroscopy (TP-DRIFTS). The above-mentioned TPD profiles provided the information about the desorption products. To get more information about the surface species formed on ETB catalysts, TP-DRIFTS of Zn−Y/Beta was performed. After saturation with ethanol at 303 K, the catalyst was purged with flowing argon to remove the gas phase and weakly adsorbed ethanol molecules. Subsequently, the cell temperature was gradually increased from 303 to 723 K with a heating rate of 5 K/min. The DRIFT spectra obtained after subtraction of the background (bare catalyst) are shown in Figure 5.

DOI: 10.1021/acscatal.8b00014
ACS Catal. 2018, 8, 2760−2773

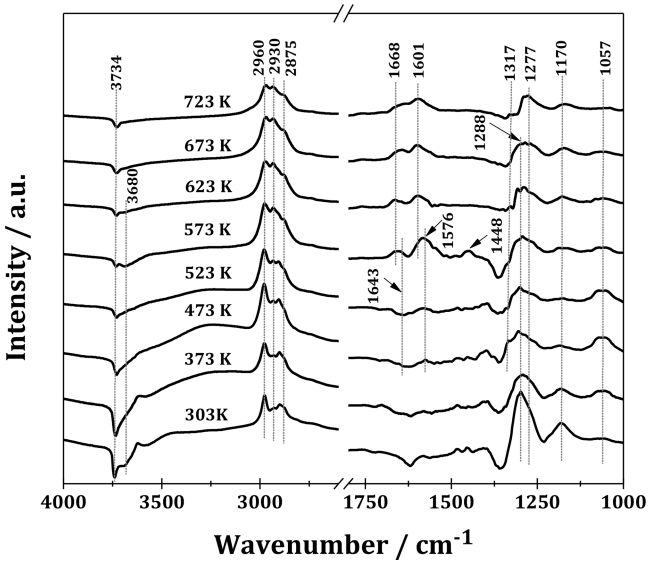

Figure 5. Temperature-programmed DRIFTS spectra obtained during the ethanol to butadiene conversion over Zn−Y/catalyst. Reaction conditions: WHSV = 1.0 h^{-1}, temperature of T = 303−723 K.

At T = 303 K, large negative bands at 3680−3734 cm^{-1} due to the interaction of ethanol with surface OH groups occurred in the spectra. In addition, the bands of two different types of adsorbed ethanol could be observed: (i) bands at 1170 and 1057 cm^{-1} due to two types of surface ethoxy groups (products of the ethanol dehydration) coordinated at different surface sites,[40,41] and (ii) a large band at 1270−1288 cm^{-1} caused by ethanol molecules, which are strongly adsorbed at Lewis acid sites. The occurrence of the latter band and the absence of a broad band at 3000−3500 cm^{-1} indicate that this species should be chemisorbed via the oxygen lone pair at Lewis acid sites, which is supported by previous FTIR studies of ethanol adsorption.[23,41−44] Bands at 2960, 2930, and 2875 cm^{-1} were caused by $CH_3\nu(a)$, $CH_2\nu(a)$, and $CH_3\nu(s)$ stretching modes.[42,45]

With increasing reaction temperature, a gradual decrease of the negative bands at 3680−3734 cm^{-1} occurred, indicating the partial desorption and/or reaction of surface-bound ethanol. Meanwhile, a decrease of the band intensities at 1270−1288, 1170, and 1057 cm^{-1} indicated the desorption and/or the reaction of the chemisorbed ethanol and surface ethoxy groups. This is in line with the ethanol TPD profiles (Figure 4). When the temperature increased to 473 K, new bands appeared at 1643 and 1576 cm^{-1}. These bands showed a blue-shift to ∼1668 and 1601 cm^{-1}, when the temperature further increased to over 573 K. According to previous study,[46,47] the above-mentioned bands could be assigned to $\nu(C=O)$ and $\nu(C=C)$ vibration modes of coupling products, e.g., crotonaldehyde and other large molecules. This assignment was supported by the adsorption of pure crotonaldehyde at 623 K, which led to the occurrence of two bands at 1670 and 1600 cm^{-1} (SI Figure S2). An emerging band at 1317 cm^{-1} occurred at over 473 K. This band together with the band at ∼1600 cm^{-1} could be explained by enolate species,[46] which was expected to be the primary intermediate in the formation of coupling products via the Aldol condensation, such as crotonaldehyde and crotyl alcohol. These finding suggest that the aldol condensation occurs according to the mechanism shown in Scheme 1, in good agreement with the results of the ethanol TPD profiles, i.e., the desorption of crotonaldehyde and crotyl alcohol started to increase at 473 K. However, these enolate species were not stable and, therefore, could not be detected in the desorption products. Moreover, an additional band appears at 1448 cm^{-1} with the temperature increasing to 573 K. Because of the absence of a C−H stretching band at ∼3025 cm^{-1}, the formation of crotyl alcohol species could be excluded.[2,48] Therefore, this band should be attributed to acetate species, which were probably formed via a Cannizzaro reaction of acetaldehyde, which was also supported by the results of pure acetaldehyde conversion (vide infra; Figure 7).[46]

To summarize these TP-DRIFTS experiments, we conclude that ethanol strongly adsorbs at the Lewis acid sites of the Zn−Y/Beta catalysts and can be converted to intermediates with increasing reaction temperature. The appearance of enolate intermediates together with coupling products indicates that the aldol condensation reaction occurs during the ethanol conversion process, which is in line with the mechanistic hypothesis as shown in Scheme 1. However, no characteristic DRIFTS bands for acetaldehyde were observed in this experiment. Hence, the acetaldehyde can easily desorb from the surface or is rapidly converted to other intermediates under reaction conditions. Additionally, the high concentrations of butadiene determined in the TPD profiles cannot been observed in the DRIFTS spectra. It indicates a fast desorption of butadiene from the gas−solid interface after its formation, in agreement with the previous report of Hermans and co-workers.[2]

3.5. Temperature-Programmed Surface Reaction (TPSR) Experiments. In Figure 6, the TPSR profiles obtained for Y/Beta, Zn/Beta, and Zn−Y/Beta under a constant ethanol flow are shown. For the Zn/Beta catalyst (Figure 6a), the ethanol curve started to decrease at 450 K, while simultaneously the acetaldehyde and hydrogen curves slopped upward. This hints to the occurrence of the ethanol dehydrogenation reaction ($CH_3CH_2OH \rightarrow CH_3CHO + H_2$). Additionally, the increase of the hydrogen curve was much stronger than that of acetaldehyde, indicating that a significant portion of acetaldehyde was involved in the subsequent reaction. With the increase of the reaction temperature to 450 K, crotonaldehyde, crotyl alcohol, and butadiene started to appear and exhibited the same variation trend. Meanwhile, a slight increase of water could also be observed, indicating the occurrence of a dehydration reaction. According to the proposed mechanism (Scheme 1), this can be due to the formation of crotonaldehyde and butadiene, i.e., an acetaldol dehydration to crotonaldehyde and a crotyl alcohol dehydration to butadiene.

For the Y/Beta catalyst, the variation trends of acetaldehyde and hydrogen were in opposite, that is, the acetaldehyde signal started to decrease with increasing hydrogen signal. This means that the reaction rate of the aldol condensation over Y/Beta catalyst is much higher than that of the ethanol dehydrogenation. Interestingly, in the temperature range of 423−648 K, the signal of crotyl alcohol was much higher than that of crotonaldehyde, while for Zn/Beta catalyst, the crotyl alcohol evolution nearly overlapped with that of crotonaldehyde. It implies that the Y/Beta catalyst is more active than Zn/Beta in the MPV reduction, in good agreement with the ethanol TPD results (Figure 4). Furthermore, the initial butadiene formation temperature for Y/Beta (395 K) was much lower than for Zn/Beta (455 K), indicating that Y/Beta could significantly reduce the activation energy barrier of the ETB conversion, which again fits well with the ethanol TPD results (Figure 4).

DOI: 10.1021/acscatal.8b00014
ACS Catal. 2018, 8, 2760−2773

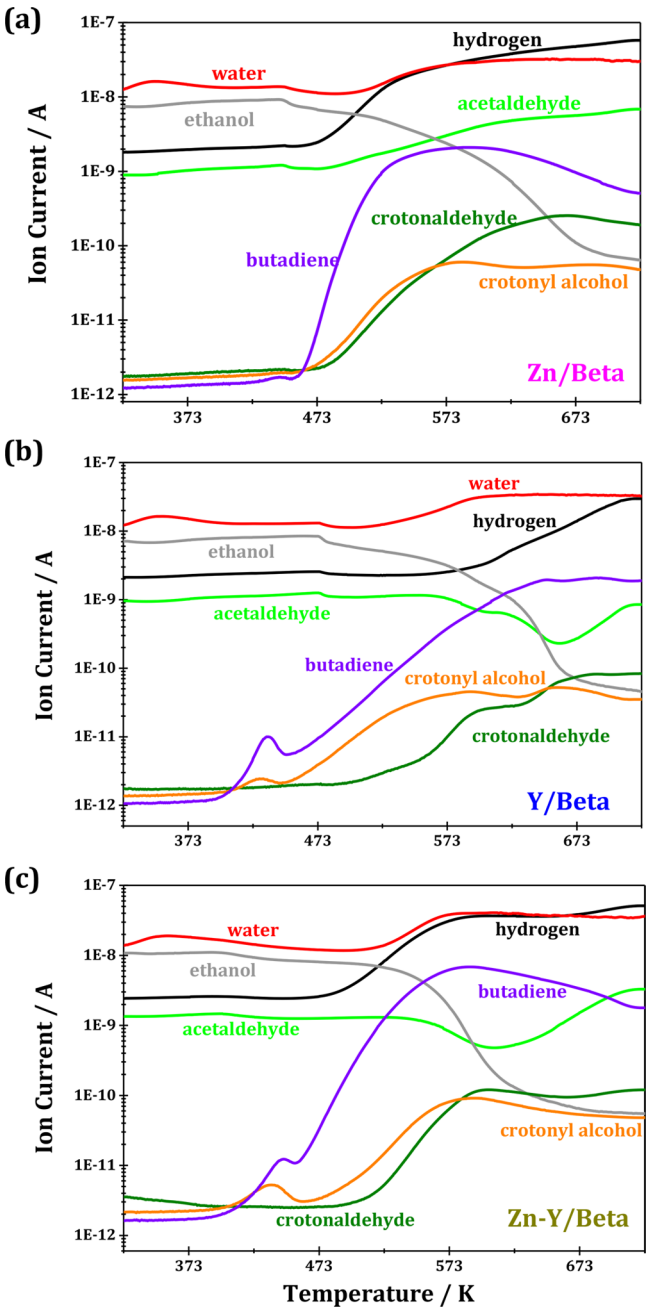

Figure 6. Temperature-programmed surface reaction (TPSR) profiles in the ethanol to butadiene conversion under a constant ethanol stream over the different catalysts: (a) Zn/Beta, (b) Y/Beta, and (c) Zn−Y/Beta. Reaction conditions: WHSV = 1.0 h^{-1}, reaction temperature of T = 623 K.

Butadiene and crotyl alcohol both exhibited a similarly small peak at ~423 K, revealing the close connection between butadiene and crotyl alcohol, namely, butadiene being the dehydration product of crotyl alcohol.

For the Zn−Y/Beta catalyst, the variation trend of the above-mentioned intermediates was somewhat different to that of Zn/Beta or Y/Beta. Typically, the variation trend of hydrogen over the Zn−Y/Beta catalyst was similar to that over Zn/Beta, while the variation trends of crotonaldehyde, crotyl alcohol, and butadiene were more similar to those over Y/Beta. On the other side, the low initial butadiene formation temperature for Zn−Y/Beta was similar to that observed for Y/Beta. According to these results, we conclude that the roles of Zn and Y species in the ETB conversion can be well combined in the Zn−Y/Beta catalyst, i.e., the good dehydrogenation activity of Zn species and the excellent activity of Y species in the aldol condensation and MPV reduction can be well preserved in the Zn−Y/Beta catalyst. This explains the high yields of butadiene achieved over the Zn−Y/Beta catalyst (Figure 3).

3.6. Online Mass-Spectrometry Modulation Experiments with Ethanol and Acetaldehyde. To obtain deeper insight into the reaction mechanism and to clarify the role of acetaldehyde in the ETB conversion, online modulation experiments with ethanol and acetaldehyde were performed for the three catalysts under study (Figure 7). For pure ethanol conversion, the signal intensities of the intermediates formed over Y/Beta were much lower than those over Zn/Beta and Zn−Y/Beta, especially for hydrogen, indicating that Y/Beta had the lower dehydrogenation activity, which is in line with the ethanol TPD and TPSR experiments. A direct comparison of the initial 5 min of the ETB conversion over the three catalysts under study (Figure S3) indicates that the ethanol dehydrogenation to acetaldehyde is the first reaction step. In addition, with the progress of the ETB conversion, the intensity of the crotonaldehyde signal for Zn/Beta was becoming higher than that of crotyl alcohol, while for Y/Beta and Zn−Y/Beta, the variation trends were in opposite. This fits well with the ethanol TPD and TPSR experiments, implying that Y/Beta is more active in the MPV reduction than Zn/Beta.

With acetaldehyde cofeeding (ethanol:acetaldehyde = 4:1), the crotonaldehyde signals significantly increased for all the three catalysts. Hence, the crotonaldehyde is preferentially formed in the presence of acetaldehyde, supporting the route of acetaldehyde aldol condensation to crotonaldehyde. For Y/Beta and Zn−Y/Beta, the intensities of the crotonaldehyde signals were much higher than that of Zn/Beta after the acetaldehyde co-feeding. This means that Y/Beta has a higher aldol condensation activity. In addition, with the presence of acetaldehyde, the ethanol dehydrogenation could be suppressed, which led to a decrease of the hydrogen signal. This should be due to the occupying of active sites by acetaldehyde, which accordingly decreases the number of empty surface sites for the ethanol dehydrogenation.

With increasing acetaldehyde contents in the feed (ethanol:acetaldehyde = 1:1), larger slopes of the intermediate signals occurred for all of the three catalysts under study, indicating that the reaction equilibrium between ethanol, intermediates, and reaction products could be significantly accelerated with the presence of acetaldehyde. This may provide an indirect evidence for the participation of acetaldehyde as an intermediate during the ETB conversion. Interestingly, when acetaldehyde was fed alone, all of the above-mentioned intermediates with similar variation trends could also be formed over all of the three catalysts under study, being inconsistent with the proposed mechanism (Scheme 1) as no ethanol was present. In fact, ethanol and acetic acid could also be observed in the MS spectra, which may be due to the Cannizzaro reaction of acetaldehyde.[46] Therefore, crotonaldehyde, crotyl alcohol, and butadiene can be also formed over the catalysts under study via conversion of pure acetaldehyde.

To summarize these experimental observations, we conclude that the ethanol dehydrogenation to acetaldehyde is the first reaction step of the ETB conversion. With the acetaldehyde co-feeding, the formation of crotonaldehyde is strongly promoted, hinting at the occurrence of the acetaldehyde aldol con-

DOI: 10.1021/acscatal.8b00014
ACS Catal. 2018, 8, 2760−2773

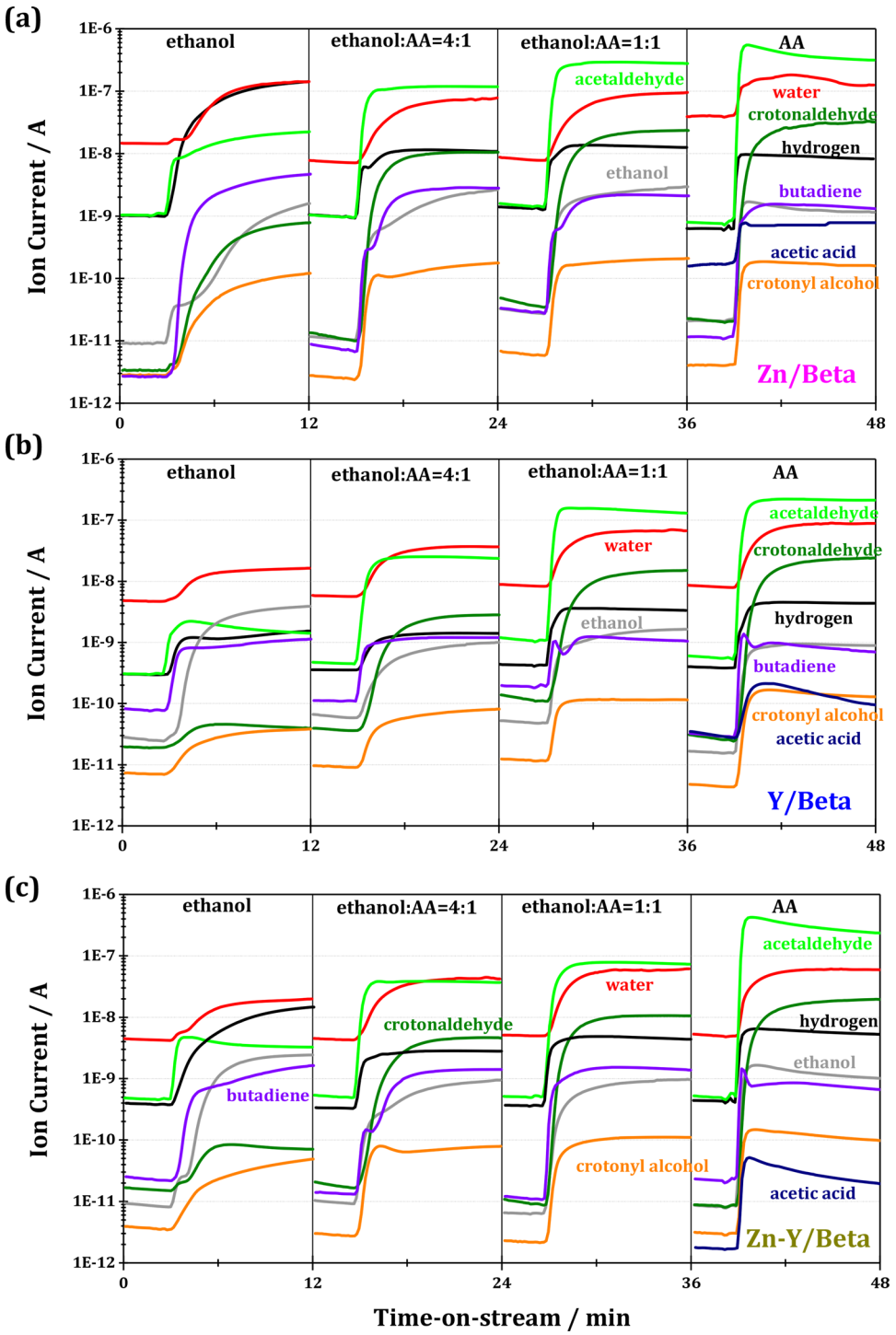

Figure 7. Modulation experiments with different proportions of ethanol and acetaldehyde (AA) over the catalysts: (a) Zn/Beta, (b) Y/Beta, and (c) Zn−Y/Beta. Reaction conditions: WHSV = 1.0 h^{-1}, reaction temperature of T = 623 K.

densation reaction. In addition, Zn and Y species both exhibit a dehydrogenation and aldol condensation activity, but Zn species are characterized by a higher dehydrogenation activity and lower aldol condensation activity than Y species.

3.7. Online Mass-Spectrometry Modulation Experiments with Ethanol and Crotonaldehyde. According to the proposed reaction route in Scheme 1, crotonaldehyde is involved in the MPV reduction. To investigate the roles of Zn and Y species in the MPV reduction, online modulation experiments with ethanol and crotonaldehyde were performed with the three catalysts under study (Figure 8). With crotonaldehyde co-feeding, reaction intermediates with similar variation trends could be observed for all three catalysts. In accordance with the above-mentioned results, the hydrogen signal observed for Y/Beta was much lower than that for Zn/Beta or Zn−Y/Beta due to the lower dehydrogenation activity. Interestingly, in comparison with the pure ethanol conversion, the butadiene signal observed for Y/Beta was significantly promoted with crotonaldehyde cofeeding, even a little higher than that for Zn/Beta. On the other hand, the signal of the

DOI: 10.1021/acscatal.8b00014
ACS Catal. 2018, 8, 2760−2773

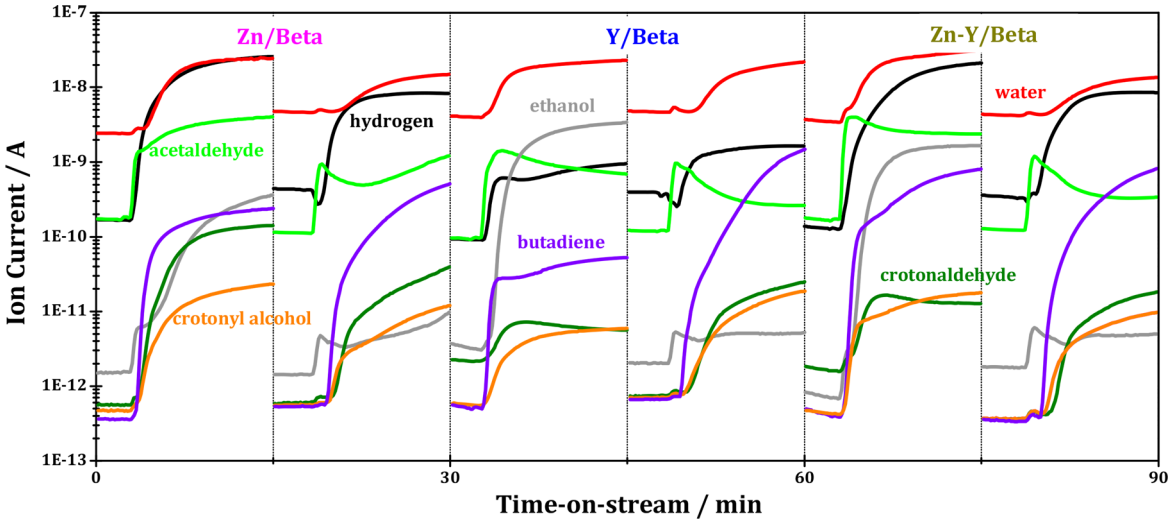

Figure 8. Modulation experiments about crotonaldehyde and ethanol over the different catalysts (left: ethanol; right: ethanol and crotonaldehyde cofeeding). Reaction conditions: WHSV = 1.0 h^{-1}, reaction temperature of T = 623 K.

unconverted crotonaldehyde for Y/Beta was lower than that for Zn/Beta. Obviously, the increase in the butadiene signal suggests that a MPV reduction occurs with the presence of crotonaldehyde. The lower signal of unconverted crotonaldehyde for Y/Beta indicates its higher activity in the MPV reduction.

According to the observations from crotonaldehyde cofeeding experiments, we can state that the MPV reduction reaction occurs with the presence of ethanol and crotonaldehyde. Meanwhile, Y species are more active than Zn species in the MPV reduction reaction.

3.8. In Situ Diffuse Reflectance Infrared Fourier Transform Spectroscopy (in situ-DRIFTS). To further compare surface intermediates and gas-phase products formed during the ETB conversion over the different catalysts under study, in situ DRIFTS experiments were performed (Figure 9). In the spectra of all the three catalysts under study, there are two negative bands at high wavenumbers of 3680−3734 cm^{-1}, which hint at an interaction of ethanol with OH groups, i.e., Si-OH and Zn- or Y-OH groups. Bands at about 2875−2960 cm^{-1}, due to $CH_{3\nu(a)}$, $CH_{2\nu(a)}$, and $CH_{3\nu(s)}$ stretching modes of the ethanol molecules, are also similar for all the three catalysts. In addition, similar bands at low wavenumbers of 1060−1280 cm^{-1}, due to ethanol molecules coordinated at Lewis acid sites and ethoxy groups, also occurred in the spectra of all three catalysts. These observations reveal an interaction between absorbed ethanol and Zn or Y species.

However, there are significant differences in the IR bands observed for Zn/Beta and Y/Beta in the range of 1700−1500 cm^{-1}. For Zn/Beta, a weak band at 1705 cm^{-1} due to acetaldehyde occurred during the initial process of the ethanol conversion, but it gradually disappeared with the progress of the ethanol conversion. Simultaneously, acetate species (1448 cm^{-1}) and coupling products, such as crotonaldehyde and other large intermediates (bands at 1601, 1668, and 2734 cm^{-1}), were formed. It indicates that the acetaldehyde formed during the initial period of the ethanol conversion can be rapidly involved in a subsequent aldol condensation reaction. In this context, acetaldehyde should be regarded as the initial intermediate.[46,49] But for Y/Beta, nearly no bands of the above-mentioned intermediate could be observed in the same wavenumbers range, which disagrees with the TPD and TPSR results. This may be due to its lower ethanol to butadiene activity, as shown in Figure 3, and, therefore, traces of intermediates could be rapidly converted or desorb from the Y sites. For Zn−Y/Beta, similar bands as those observed for Zn/Beta, but with higher intensities occurred in the spectra, hinting at a synergism of Zn and Y species, which promoted the activity in the ETB conversion.

To get more information about the role of acetaldehyde in the ETB conversion, in situ DRIFTS experiments during cofeeding of acetaldehyde and ethanol were performed, and the corresponding spectra are shown in Figure 10. In comparison with the spectra recorded during the conversion of pure ethanol, more bands of unconverted acetaldehydes at 2700, 1760, and 1705 cm^{-1} were observed for all the three catalysts. Interestingly, two new bands at ∼3020 and 3070 cm^{-1} also appeared after the acetaldehyde cofeeding. According to the previous report of Hermans and co-workers,[2] these bands could be assigned to $-CH{=}CH_2$ groups of butadiene or precursors of butadiene, e.g., crotyl alcohol. However, according to the above DRIFTS experiments performed during conversion of pure ethanol, we know that the crotyl alcohol intermediates can be rapidly converted to butadiene, and butadiene desorbs easily from the catalyst surface. Therefore, the appearance of these two species in the DRIFTS spectra indicates an easy formation of crotyl alcohol or butadiene in the presence of acetaldehyde. In other words, acetaldehyde plays a vital role in the ETB conversion. In addition, the appearance of these intermediates on Y/Beta indicates that the aldol condensation and MPV reduction occur preferentially in the presence of acetaldehyde. Furthermore, the intensities of the bands corresponding to strongly adsorbed ethanol (1280 cm^{-1}) in Zn/Beta decreased significantly with the introduction of Y species, i.e., for the Zn−Y/Beta catalyst. This elucidates that a synergism of Zn and Y species can significantly promote the ETB conversion, in line with the catalytic results in Figure 3.

3.9. Mechanistic Interpretation. As a very demanding reaction, the ETB conversion involves several key reaction steps, and each reaction step is catalyzed by a certain type of functional site. According to recent studies, Ag promoted Zr-Beta or Ta-Beta catalysts could also exhibit good activity in the ETB conversion.[20,22,31,32] For discussing the difference in the reaction mechanism, the properties of the Zn−Y/Beta and Ag−

DOI: 10.1021/acscatal.8b00014
ACS Catal. 2018, 8, 2760−2773

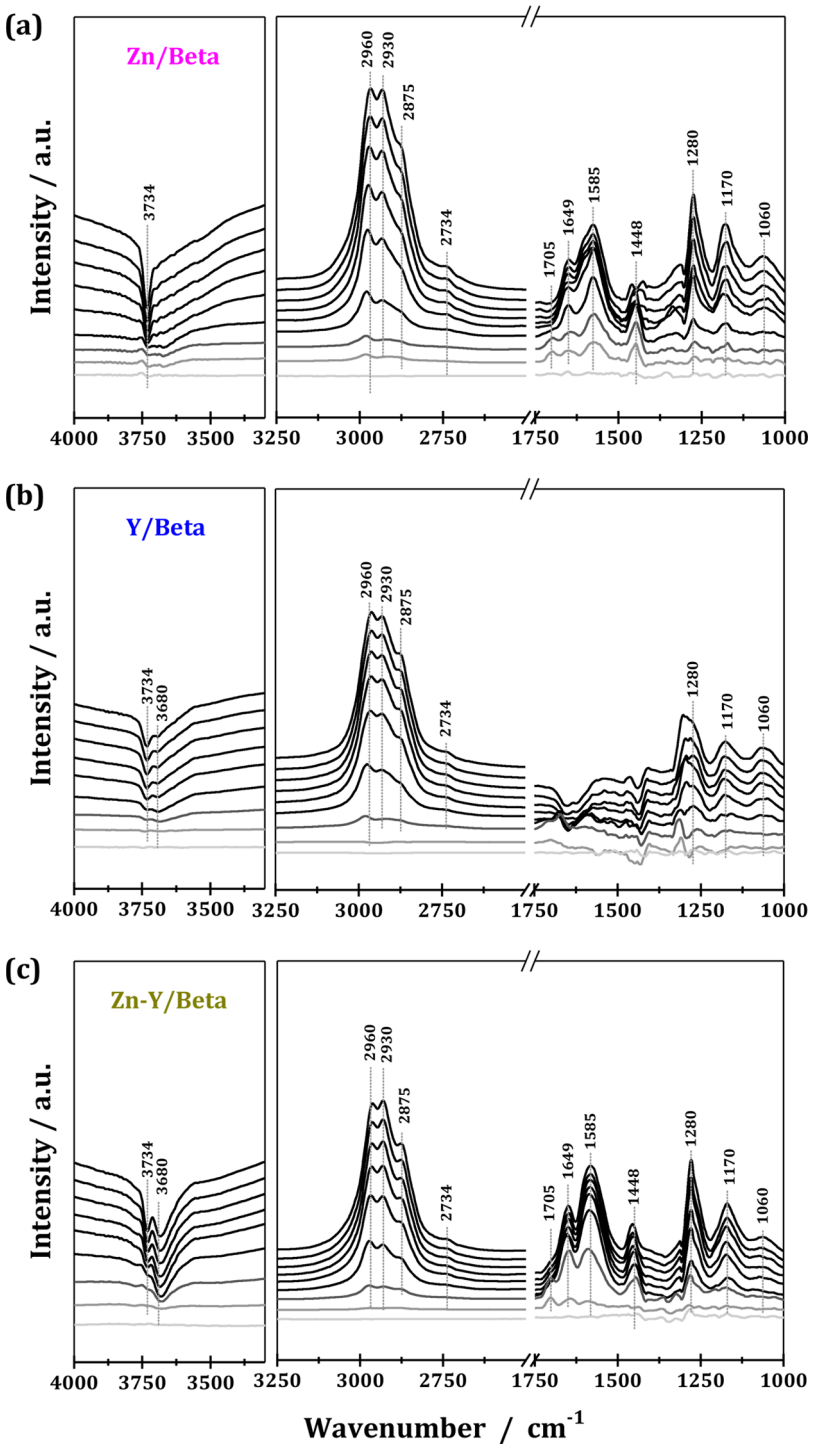

Figure 9. In situ FTIR spectra recorded during the ethanol conversion over Zn/Beta (a), Y/Beta (b), and Zn−Y/Beta (c) up to TOS = 60 min. Reaction conditions: WHSV = 1.0 h^{-1}, reaction temperature of T = 623 K.

Zr/Beta catalysts are first compared. The most significant difference between these two catalyst systems lies in the nature of the active sites and their interactions. For Zn−Y/Beta, the Zn and Y precursors were simultaneously introduced into [Si]Beta, and they can randomly interact with the silanols of [Si]Beta during the dry impregnation process. Because four silanols exist in adjacent positions in [Si]Beta (SiOH nest), the probability of the coexistence of Zn and Y in this region is very high. Upon calcination, the Zn and Y species in adjacent positions undergo rearrangements, leading to the formation of Zn−Y pairs at zeolite framework defects (SI Scheme S1).[32] In contrast, for the Ag doped Zr-Beta, the Ag species were introduced after the preparation of Zr-Beta, i.e., the Zr species were at first incorporated and could occupy hydroxyl nest. This leads to the lower probability of their close contact in the same hydroxyl nests (SI Scheme S2). Therefore, the reaction intermediates formed on the Zn−Y/Beta catalyst during the ETB conversion have a much higher chance for further reaction to produce the final products rather than escape as unwanted byproduct.

DOI: 10.1021/acscatal.8b00014
ACS Catal. 2018, 8, 2760−2773

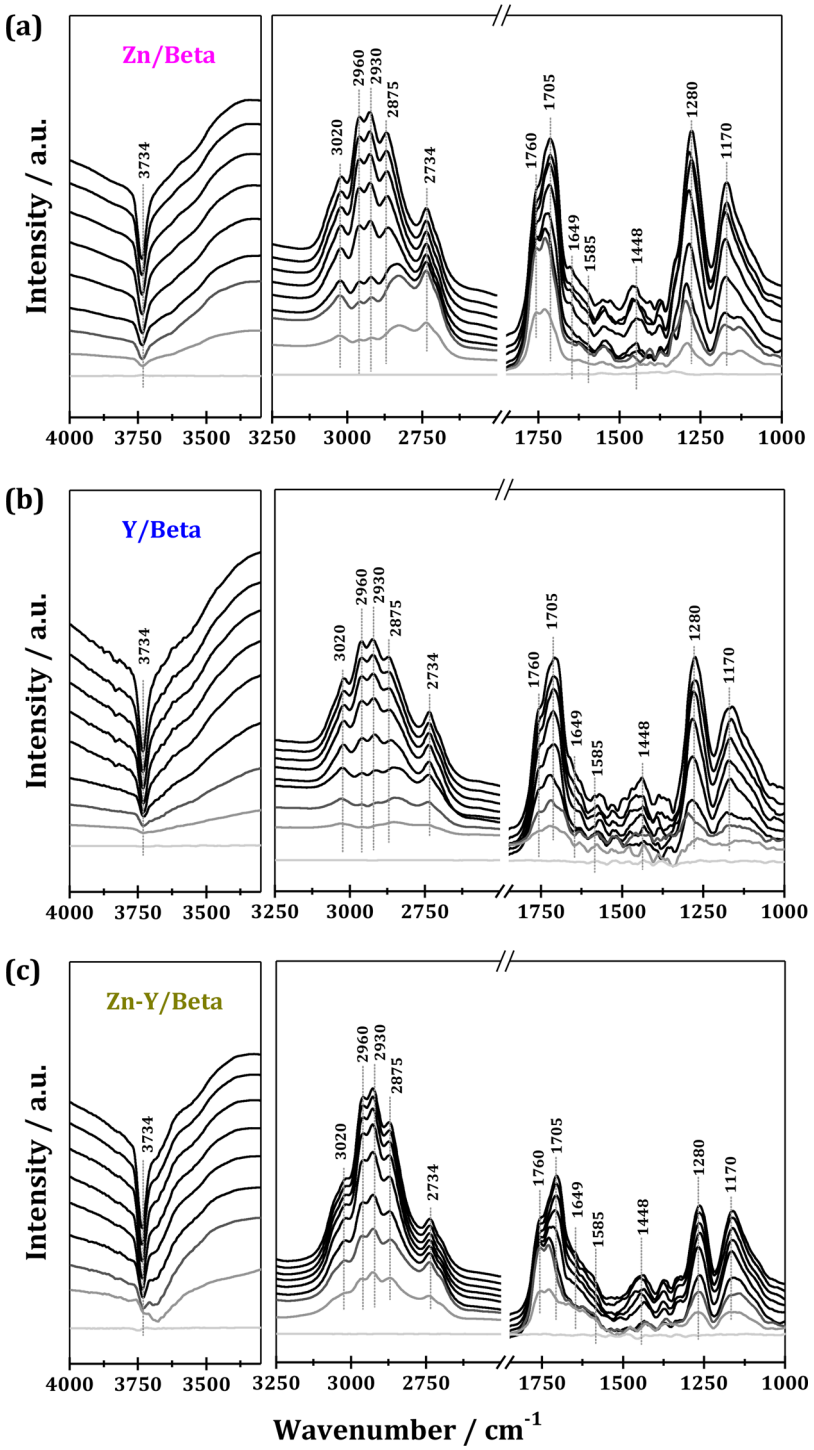

Figure 10. In situ FTIR spectra recorded during the ethanol conversion with the cofeeding of acetaldehyde (50 vol %:50 vol %) over Zn/Beta (a), Y/Beta (b), and Zn−Y/Beta (c) up to TOS = 60 min. Reaction conditions: WHSV = 1.0 h^{-1}, reaction temperature of T = 623 K.

Considering all the information obtained from the catalytic and spectroscopic investigations, we can summarize the overall reaction mechanism of the ETB conversion over the bifunctional Zn−Y/Beta catalyst, as shown in Scheme 2. According to the previous studies of Ivanova and Hermans,[30,31,50] ethanol dehydrogenation to acetaldehyde only happens at Ag sites but not at Lewis acid sites of the Ag/Zr-Beta catalyst. In the present study, however, with the presence of strongly adsorbed ethanol molecules at Lewis acid sites (Figure 5), i.e., Zn and Y species, the ethanol dehydrogenation can happen both at these two metal species. Additionally, with the coexistence of Zn and Y species in the bifunctional Zn−Y/Beta catalyst, the ethanol dehydrogenation to acetaldehyde dominantly occurs on Zn sites due to their higher dehydrogenation ability (Figure 4), but a role of Y species in this process cannot be excluded. Subsequently, acetaldehyde can easily desorb from the Zn sites, and a small part of these molecules can escape as reaction products (as observed both in the catalytic results in Figure 3 and the TPD and TPSR results in Figures 6 and 7), while others are further involved in the aldol condensation reaction to

DOI: 10.1021/acscatal.8b00014
ACS Catal. 2018, 8, 2760−2773

Scheme 2. Proposed Reaction Mechanism of Ethanol to Butadiene over Bifunctional Zn−Y/Beta Catalyst

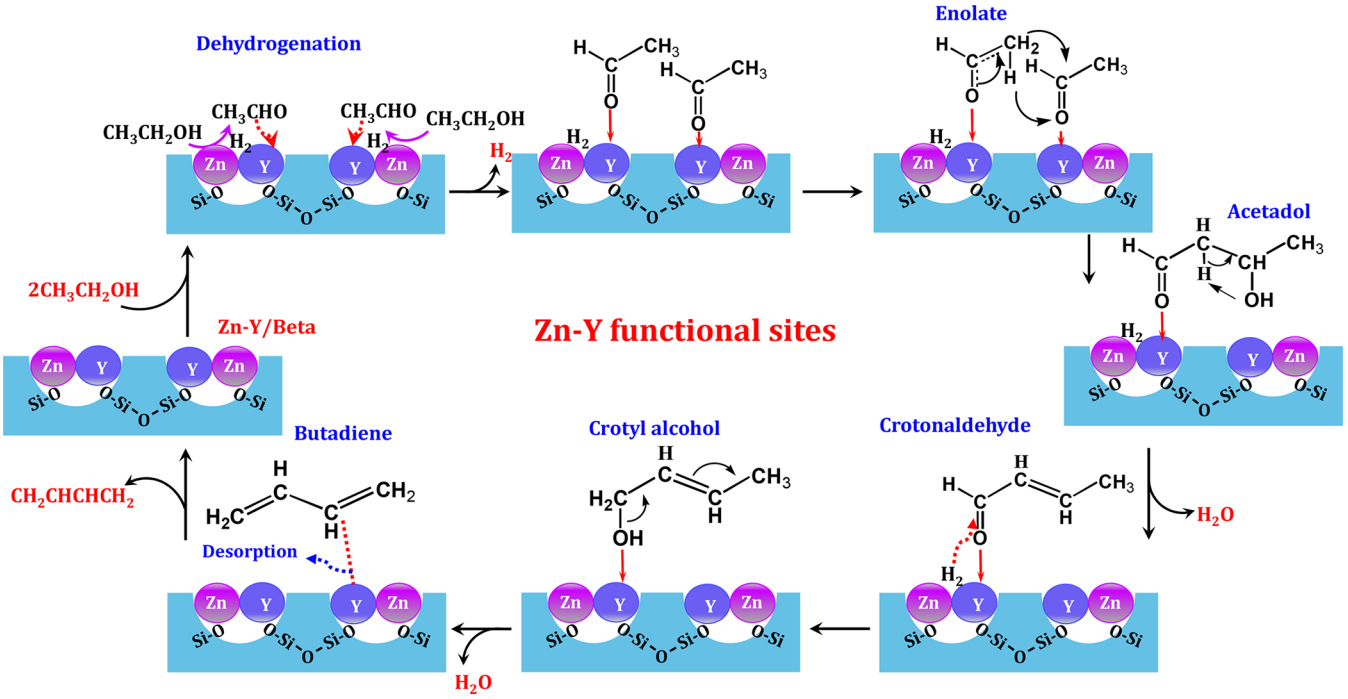

produce crotonaldehyde on the same Zn sites or neighboring Y sites. Meanwhile, hydrogen atoms can desorb as gaseous H_2 (as supported by ethanol TPD profiles in Figure 4 and TPSR profiles in Figure 6) or remain on the surface until the MPV reduction occurs. This is in line with the two catalytic cycles for the Ag promoted Zr-Beta catalyst, proposed by Sushkevich and Ivanova.[30]

Besides the above-mentioned dehydrogenation ability, Zn and Y species are also active in the aldol condensation reaction and MPV reduction (Figures 4 and 6), which is similar like the previous reports of the Zn/SiO_2 catalyst.[51] The redox sites of the Zn/SiO_2 catalyst can significantly increase the rate of ethanol dehydrogenation. On the other side, the Lewis acidity of Zn species interacting with the zeolite support can also promote the aldol reaction and MPV reaction in the ETB reaction. In the present study, the activity of Zn and Y species in the ETB conversion are also responsible for the redox properties and/or the Lewis acidity of the modified Beta zeolite, as evidenced by ^1H and ^{13}C MAS NMR investigations of adsorbed probe molecules (Figures 1 and 2).

However, with the coexistence of Zn and Y species in the bifunctioanl Zn−Y/Beta catalyst, the aldol condensation mainly happens at the Y species due to their higher condensation activity, as indicated by the co-feeding experiments (Figures 7 and 8) and the ^{13}C MAS NMR measurements of adsorbed acetone-2-^{13}C adsorption (Figure 2). Similar to the previous study of acetaldehyde aldol coupling over Sn/Beta[52,53] and $MgO-SiO_2$ catalysts,[9] an enolization step is involved in this coupling process because enolate species can be observed in the DRIFTS spectra (Figure 5). This is different from the acetaldehyde coupling over Ta-Beta investigated by Hermans and co-workers,[2] as enolate species are absent in their FTIR spectra. Thereafter, the coupling product crotonaldehyde is hydrogenated to crotyl alcohol on Y sites in the presence of H_2, which is generated on Zn sites via ethanol dehydrogenation. At last, butadiene is produced via a crotyl alcohol dehydration on Y or Zn sites or weakly acidic SiOH groups.[54,55] In addition, the participation of Zn species in the aldol condensation, MPV reduction, and butadiene formation cannot be excluded, and a synergistic action of Zn and Y species in these reactions can efficiently suppress formation of unwanted intermediates and, therefore, promote the butadiene selectivity. This is also in line with the previous reports of Zn−La−Zr−Si oxide catalysts,[56] where zinc-containing sites promoted the rate of ethanol dehydrogenation to acetaldehyde while lanthanum-containing sites and zirconium-containing sites promoted the rates of the aldol condensation and MPV reduction.

The proposed mechanism indicates that for the rational design of an eligible catalyst for an industrial one-step ETB process, two different types of surface sites should be well balanced. Here, the active Zn and Y sites in the present bifunctional catalysts mainly exist as well-distributed metal pairs confined in zeolite pores rather than incorporated into the framework. Therefore, the creation of Lewis acidity is not limited to framework heteroatoms, like Zr and Ta, and this finding provides us with new possibilities for versatile ETB catalysts in future.

4. CONCLUSIONS

The reaction mechanism of the ETB conversion over a bifunctional Zn−Y/Beta catalyst is elucidated and the roles of the Zn and Y species in the reaction are clarified. Complementary methods, ethanol TPD, TPSR, and in situ DRIFTS, reveal that the ETB conversion over Zn−Y/Beta catalyst mainly proceeds in the following steps, i.e., first ethanol dehydrogenation to acetaldehyde, acetaldehyde coupling to crotonaldehyde, followed by MPV reduction of crotonaldehyde to crotyl alcohol, and finally crotyl alcohol dehydration to butadiene.

Different from previous studies of Ta-Beta and Zr-Beta catalysts, an enolization step is involved in the coupling reaction under study. Lewis acidic Zn and Y species are active in the

DOI: 10.1021/acscatal.8b00014
ACS Catal. 2018, 8, 2760−2773

ETB conversion, and the major difference between these two species lies in their specific activity, i.e., Zn species exhibit the higher dehydrogenation activity but lower coupling activity than Y species. After combining the two species in one catalyst (Zn−Y/Beta), a synergistic effect can be well embodied and a high selectivity to butadiene is achieved. The coexistence of neighboring Zn and Y species in the Beta structure can increase the chance of the intermediates to react with each other on these sites to generate butadiene rather than escape as unwanted byproducts. These results provide fundamental guidelines to bifunctional catalysts for cascade transformation of ethanol to butadiene.

■ ASSOCIATED CONTENT

Supporting Information

The Supporting Information is available free of charge on the ACS Publications website at DOI: 10.1021/acscatal.8b00014.

Additional catalyst characterization, modulation experiment, and in situ FTIR data (PDF)

■ AUTHOR INFORMATION

Corresponding Authors

*L.L.: E-mail, lild@nankai.edu.cn.
*W.D.: E-mail, weilidai@nankai.edu.cn.

ORCID

Weili Dai: 0000-0001-5752-0662
Michael Hunger: 0000-0002-1870-2743
Landong Li: 0000-0003-0998-4061

Notes

The authors declare no competing financial interest.

■ ACKNOWLEDGMENTS

This work was supported by the National Natural Science Foundation of China (grant nos. 21722303, 21573113, 21421001), Municipal Natural Science Foundation of Tianjin (16JCQNJC04900), and 111 Project (B18030). Furthermore, M.H. is grateful for financial support by Deutsche Forschungsgemeinschaft.

■ REFERENCES

(1) Angelici, C.; Weckhuysen, B. M.; Bruijnincx, P. C. A. Chemocatalytic Conversion of Ethanol into Butadiene and Other Bulk Chemicals. *ChemSusChem* **2013**, *6*, 1595−1614.

(2) Müller, P.; Burt, S. P.; Love, A. M.; McDermott, W. P.; Wolf, P.; Hermans, I. Mechanistic Study on the Lewis Acid Catalyzed Synthesis of 1,3-Butadiene over Ta-BEA Using Modulated Operando DRIFTS-MS. *ACS Catal.* **2016**, *6*, 6823−6832.

(3) Patel, A. D.; Meesters, K.; den Uil, H.; de Jong, E.; Blok, K.; Patel, M. K. Sustainability Assessment of Novel Chemical Processes at Early Stage: Application to Biobased Processes. *Energy Environ. Sci.* **2012**, *5*, 8430−8444.

(4) White, W. C. Butadiene Production Process Overview. *Chem.-Biol. Interact.* **2007**, *166*, 10−14.

(5) Makshina, E. V.; Dusselier, M.; Janssens, W.; Degreve, J.; Jacobs, P. A.; Sels, B. F. Review of Old Chemistry and New Catalytic Advances in the on-Purpose Synthesis of Butadiene. *Chem. Soc. Rev.* **2014**, *43*, 7917−7953.

(6) Sun, J.; Wang, Y. Recent Advances in Catalytic Conversion of Ethanol to Chemicals. *ACS Catal.* **2014**, *4*, 1078−1090.

(7) Pomalaza, G.; Capron, M.; Ordomsky, V.; Dumeignil, F. Recent Breakthroughs in the Conversion of Ethanol to Butadiene. *Catalysts* **2016**, *6*, 203−237.

(8) Taifan, W. E.; Yan, G.; Baltrusaitis, J. Surface Chemistry of MgO/SiO_2 Catalysts during the Ethanol Catalytic Conversion to 1,3-Butadiene: in situ DRIFTS and DFT Study. *Catal. Sci. Technol.* **2017**, *7*, 4648−4668.

(9) Ochoa, J. V.; Bandinelli, C.; Vozniuk, O.; Chieregato, A.; Malmusi, A.; Recchi, C.; Cavani, F. An Analysis of the Chemical, Physical and Reactivity Features of MgO−SiO_2 Catalysts for Butadiene Synthesis with the Lebedev Process. *Green Chem.* **2016**, *18*, 1653−1663.

(10) Zhu, Q.; Wang, B.; Tan, T. Conversion of Ethanol and Acetaldehyde to Butadiene over MgO−SiO_2 Catalysts: Effect of Reaction Parameters and Interaction between MgO and SiO_2 on Catalytic Performance. *ACS Sustainable Chem. Eng.* **2017**, *5*, 722−733.

(11) Da Ros, S.; Jones, M. D.; Mattia, D.; Schwaab, M.; Barbosa-Coutinho, E.; Rabelo-Neto, R. C.; Bellot Noronha, F.; Pinto, J. C. Microkinetic Analysis of Ethanol to 1,3-Butadiene Reactions over MgO-SiO_2 Catalysts Based on Characterization of Experimental Fluctuations. *Chem. Eng. J.* **2017**, *308*, 988−1000.

(12) Chung, S.-H.; Angelici, C.; Hinterding, S. O. M.; Weingarth, M.; Baldus, M.; Houben, K.; Weckhuysen, B. M.; Bruijnincx, P. C. A. Role of Magnesium Silicates in Wet-Kneaded Silica−Magnesia Catalysts for the Lebedev Ethanol-to-Butadiene Process. *ACS Catal.* **2016**, *6*, 4034−4045.

(13) Makshina, E. V.; Janssens, W.; Sels, B. F.; Jacobs, P. A. Catalytic Study of the Conversion of Ethanol into 1,3-Butadiene. Catal. *Catal. Today* **2012**, *198*, 338−344.

(14) Janssens, W.; Makshina, E. V.; Vanelderen, P.; De Clippel, F.; Houthoofd, K.; Kerkhofs, S.; Martens, J. A.; Jacobs, P. A.; Sels, B. F. Ternary Ag/MgO-SiO_2 Catalysts for the Conversion of Ethanol into Butadiene. *ChemSusChem* **2015**, *8*, 994−1008.

(15) Han, Z.; Li, X.; Zhang, M.; Liu, Z.; Gao, M. Sol−gel Synthesis of ZrO_2−SiO_2 Catalysts for the Transformation of Bioethanol and Acetaldehyde into 1,3-Butadiene. *RSC Adv.* **2015**, *5*, 103982−103988.

(16) Sushkevich, V. L.; Palagin, D.; Ivanova, I. I. With Open Arms: Open Sites of ZrBEA Zeolite Facilitate Selective Synthesis of Butadiene from Ethanol. *ACS Catal.* **2015**, *5*, 4833−4836.

(17) Sushkevich, V. L.; Vimont, A.; Travert, A.; Ivanova, I. I. Spectroscopic Evidence for Open and Closed Lewis Acid Sites in ZrBEA Zeolites. *J. Phys. Chem. C* **2015**, *119*, 17633−17639.

(18) Chae, H. J.; Kim, T. W.; Moon, Y. K.; Kim, H. K.; Jeong, K. E.; Kim, C. U.; Jeong, S. Y. Butadiene Production from Bioethanol and Acetaldehyde over Tantalum Oxide-Supported Ordered Mesoporous Silica Catalysts. *Appl. Catal., B* **2014**, *150−151*, 596−604.

(19) Kyriienko, P. I.; Larina, O. V.; Soloviev, S. O.; Orlyk, S. M.; Dzwigaj, S. High Selectivity of TaSiBEA Zeolite Catalysts in 1,3-Butadiene Production from Ethanol and Acetaldehyde Mixture. Catal. *Catal. Commun.* **2016**, *77*, 123−126.

(20) Kyriienko, P. I.; Larina, O. V.; Soloviev, S. O.; Orlyk, S. M.; Calers, C.; Dzwigaj, S. Ethanol Conversion into 1,3-Butadiene by the Lebedev Method over MTaSiBEA Zeolites (M = Ag, Cu, Zn). *ACS Sustainable Chem. Eng.* **2017**, *5*, 2075−2083.

(21) Sushkevich, V. L.; Ivanova, I. I.; Taarning, E. Ethanol Conversion into Butadiene over Zr-containing Molecular Sieves Doped with Silver. *Green Chem.* **2015**, *17*, 2552−2559.

(22) Sushkevich, V. L.; Ivanova, I. I. Ag-Promoted ZrBEA Zeolites Obtained by Post-Synthetic Modification for Conversion of Ethanol to Butadiene. *ChemSusChem* **2016**, *9*, 2216−2225.

(23) Angelici, C.; Velthoen, M. E. Z.; Weckhuysen, B. M.; Bruijnincx, P. C. A. Effect of Preparation Method and CuO Promotion in the Conversion of Ethanol into 1,3-Butadiene over SiO_2-MgO Catalysts. *ChemSusChem* **2014**, *7*, 2505−2515.

(24) Sushkevich, V. L.; Ivanova, I. I.; Ordomsky, V. V.; Taarning, E. Design of a Metal-Promoted Oxide Catalyst for the Selective Synthesis of Butadiene from Ethanol. *ChemSusChem* **2014**, *7*, 2527−2536.

(25) Hayashi, Y.; Akiyama, S.; Miyaji, A.; Sekiguchi, Y.; Sakamoto, Y.; Shiga, A.; Koyama, T. R.; Motokura, K.; Baba, T. Experimental and Computational Studies of the Roles of MgO and Zn in Talc for the Selective Formation of 1,3-Butadiene in the Conversion of Ethanol. *Phys. Chem. Chem. Phys.* **2016**, *18*, 25191−25209.

DOI: 10.1021/acscatal.8b00014
ACS Catal. 2018, 8, 2760−2773

(26) Ochoa, J. V.; Malmusi, A.; Recchi, C.; Cavani, F. Understanding the Role of Gallium as a New Promoter of MgO-SiO_2 Catalysts for the Conversion of Ethanol into Butadiene. *ChemCatChem* **2017**, *9*, 2128−2135.
(27) Shylesh, S.; Gokhale, A. A.; Scown, C. D.; Kim, D.; Ho, C. R.; Bell, A. T. From Sugars to Wheels: The Conversion of Ethanol to 1,3-Butadiene over Metal-Promoted Magnesia-Silicate Catalysts. *ChemSusChem* **2016**, *9*, 1462−1472.
(28) Da Ros, S.; Jones, M. D.; Mattia, D.; Pinto, J. C.; Schwaab, M.; Noronha, F. B.; Kondrat, S. A.; Clarke, T. C.; Taylor, S. H. Ethanol to 1,3-Butadiene Conversion by Using ZrZn-Containing MgO-SiO_2 Systems Prepared by Co-precipitation and Effect of Catalysis Acidity Modification. *ChemCatChem* **2016**, *8*, 2376−2386.
(29) Angelici, C.; Meirer, F.; van der Eerden, A. M. J.; Schaink, H. L.; Goryachev, A.; Hofmann, J. P.; Hensen, E. J. M.; Weckhuysen, B. M.; Bruijnincx, P. C. A. Ex Situ and Operando Studies on the Role of Copper in Cu-Promoted SiO_2−MgO Catalysts for the Lebedev Ethanol-to-Butadiene Process. *ACS Catal.* **2015**, *5*, 6005−6015.
(30) Sushkevich, V. L.; Ivanova, I. I. Mechanistic Study of Ethanol Conversion into Butadiene over Silver Promoted Zirconia Catalysts. *Appl. Catal., B* **2017**, *215*, 36−49.
(31) Mueller, P.; Wang, S.-C.; Burt, S. P.; Hermans, I. Influence of Metal-Doping on the Lewis-Acid Catalyzed Production of Butadiene from Ethanol Studied by Modulated Operando DRIFTS-MS. *ChemCatChem* **2017**, *9*, 3572−3582.
(32) Dai, W.; Zhang, S.; Yu, Z.; Yan, T.; Wu, G.; Guan, N.; Li, L. Zeolite Structural Confinement Effects Enhance One-Pot Catalytic Conversion of Ethanol to Butadiene. *ACS Catal.* **2017**, *7*, 3703−3706.
(33) Lang, S.; Benz, M.; Obenaus, U.; Himmelmann, R.; Scheibe, M.; Klemm, E.; Weitkamp, J.; Hunger, M. Mechanisms of the $AlCl_3$ Modification of Siliceous Microporous and Mesoporous Catalysts Investigated by Multi-Nuclear Solid-State NMR. *Top. Catal.* **2017**, *60*, 1537−1553.
(34) Dai, W.; Sun, X.; Tang, B.; Wu, G.; Li, L.; Guan, N.; Hunger, M. Verifying the Mechanism of the Ethene-to-Propene Conversion on Zeolite H-SSZ-13. *J. Catal.* **2014**, *314*, 10−20.
(35) Gabrienko, A. A.; Arzumanov, S. S.; Toktarev, A. V.; Danilova, I. G.; Prosvirin, I. P.; Kriventsov, V. V.; Zaikovskii, V. I.; Freude, D.; Stepanov, A. G. Different Efficiency of Zn^{2+} and ZnO Species for Methane Activation on Zn-Modified Zeolite. *ACS Catal.* **2017**, *7*, 1818−1830.
(36) Lang, S.; Benz, M.; Obenaus, U.; Himmelmann, R.; Hunger, M. Novel Approach for the Characterization of Lewis Acidic Solid-State NMR Spectroscopy. *ChemCatChem* **2016**, *8*, 2031−2036.
(37) Jiang, Y.; Huang, J.; Dai, W.; Hunger, M. Solid-state Nuclear Magnetic Resonance Investigations of the Nature, Property, and Activity of Acid Sites on Solid Catalysts. *Solid State Nucl. Magn. Reson.* **2011**, *39*, 116−141.
(38) Quattlebaum, W. M.; Toussaint, W. J.; Dunn, J. T. Deoxygenation of Certain Aldehydes and Ketones: Preparation of Butadiene and styrene. *J. Am. Chem. Soc.* **1947**, *69*, 593−594.
(39) Jones, M. D. Catalytic Transformation of Ethanol into 1,3-Butadiene. *Chem. Cent. J.* **2014**, *8*, 53−58.
(40) Hussein, G. A. M.; Sheppard, N.; Zaki, M. I.; Fahim, R. B. Infrared Spectroscopic Studies of the Reactions of Alcohols over Group IVB Metal Oxide Catalysts. *J. Chem. Soc., Faraday Trans.* **1991**, *87*, 2655−2659.
(41) Hussein, G. A. M.; Sheppard, N.; Zaki, M. I.; Fahim, R. B. Infrared Spectroscopic Studies of the Reactions of Alcohols over Group IVB Metal Oxide Catalysts 3. Ethanol over TiO_2 ZrO_2 and HfO_2 and General Conclusion from Part 1 to Part 3. *J. Chem. Soc., Faraday Trans.* **1991**, *87*, 2661−2668.
(42) Dömök, M.; Tóth, M.; Raskó, J.; Erdohelyi, A. Adsorption and Reactions of Ethanol and Ethanol−water Mixture on Alumina-Supported Pt Catalysts. *Appl. Catal., B* **2007**, *69*, 262−272.
(43) Nadeem, A. M.; Waterhouse, G. I. N.; Idriss, H. The Reactions of Ethanol on TiO_2 and Au/TiO_2 Anatase Catalysts. Catal. *Catal. Today* **2012**, *182*, 16−24.
(44) Ochoa, J. V.; Trevisanut, C.; Millet, J-M. M.; Busca, G.; Cavani, F. In Situ DRIFTS-MS Study of the Anaerobic Oxidation of Ethanol over Spinel Mixed Oxides. *J. Phys. Chem. C* **2013**, *117*, 23908−23918.
(45) Birky, T. W.; Kozlowski, J. T.; Davis, R. J. Isotopic Transient Analysis of the Ethanol Coupling Reaction over Magnesia. *J. Catal.* **2013**, *298*, 130−137.
(46) Mann, A. K. P.; Wu, Z.; Calaza, F. C.; Overbury, S. H. Adsorption and Reaction of Acetaldehyde on Shape-Controlled CeO_2 Nanocrystals: Elucidation of Structure−Function Relationships. *ACS Catal.* **2014**, *4*, 2437−2448.
(47) Dandekar, A.; Baker, R. T. K.; Vannice, M. A. Carbon-Supported Copper Catalysts II. Crotonaldehyde Hydrogenation. *J. Catal.* **1999**, *184*, 421−439.
(48) Young, Z. D.; Hanspal, S.; Davis, R. J. Aldol Condensation of Acetaldehyde over Titania, Hydroxyapatite, and Magnesia. *ACS Catal.* **2016**, *6*, 3193−3202.
(49) Li, M.; Wu, Z.; Overbury, S. H. Surface Structure Dependence of Selective Oxidation of Ethanol on Faceted CeO_2 Nanocrystals. *J. Catal.* **2013**, *306*, 164−176.
(50) Sushkevich, V. L.; Ivanova, I. I.; Taarning, E. Mechanistic Study of Ethanol Dehydrogenation over Silica-Supported Silver. *ChemCatChem* **2013**, *5*, 2367−2373.
(51) Larina, O. V.; Kyriienko, P. I.; Soloviev, S. O. Ethanol Conversion to 1,3-Butadiene on ZnO/MgO−SiO_2 Catalysts: Effect of ZnO Content and MgO: SiO_2 Ratio. *Catal. Lett.* **2015**, *145*, 1162−1168.
(52) Lewis, J. D.; van de Vyver, S.; Roman-Leshkov, Y. Acid−Base Pairs in Lewis Acidic Zeolites Promote Direct Aldol Reactions by Soft Enolization. *Angew. Chem., Int. Ed.* **2015**, *54*, 9835−9838.
(53) Van de Vyver, S.; Odermatt, C.; Romero, K.; Prasomsri, T.; Román-Leshkov, Y. Solid Lewis Acids Catalyze the Carbon−Carbon Coupling between Carbohydrates and Formaldehyde. *ACS Catal.* **2015**, *5*, 972−977.
(54) Chieregato, A.; Velasquez Ochoa, J.; Bandinelli, C.; Fornasari, G.; Cavani, F.; Mella, M. On the Chemistry of Ethanol on Basic Oxides: Revising Mechanisms and Intermediates in the Lebedev and Guerbet Reactions. *ChemSusChem* **2015**, *8*, 377−388.
(55) Angelici, C.; Velthoen, M. E. Z.; Weckhuysen, B. M.; Bruijnincx, P. C. A. Influence of Acid−Base Properties on the Lebedev Ethanol-to-Butadiene Process Catalyzed by SiO_2−MgO Materials. *Catal. Sci. Technol.* **2015**, *5*, 2869−2879.
(56) Larina, O. V.; Kyriienko, P. I.; Soloviev, S. O. Effect of Lanthanum in Zn-La(-Zr)-Si Oxide Compositions on their Activity in the Conversion of Ethanol into 1,3-Butadiene. *Theor. Exp. Chem.* **2016**, *52*, 51−56.

DOI: 10.1021/acscatal.8b00014
ACS Catal. 2018, 8, 2760−2773